Civil Engineering and Applied Solutions

*Research Article*

journal homepage: ceas.journals.umz.ac.ir

CEAS Civil Engineering and Applied Solutions

# Multi-Parameter Assessment and Qualitative Zoning of Groundwater Resources to Identify Critical Quality Areas Using a GIS Approach

Milad Ghaderi Khorasgani [a], Hamed Reza Zarif Sanayei [a], Massoud Morsali [b*], Saeed Toghyani [a]

[a] *Department of Civil Engineering, University of Shahrkord, Shahrkord, Iran*

[b] *Department of Geology, Faculty of Science, University of Isfahan, Isfahan, Iran*

A R T I C L E I N F O

*Keywords:*

Groundwater quality index (GWQI)
Qualitative zoning
Groundwater resources
Chaharmahal and bakhtiari province
Principal component analysis (PCA)
Geographic information system (GIS)

*Article history:*

Received 08 July 2025
Accepted 13 July 2025
Available online 20 July 2025

A B S T R A C T

This study conducts a multi-parameter assessment of groundwater quality in Chaharmahal and Bakhtiari province, Iran, to identify critical zones and support sustainable water resource management. Groundwater, vital for potable, irrigation, and industrial needs, was evaluated using the groundwater quality index (GWQI), Principal component analysis (PCA), and geographic information systems (GIS). Data from 2015–2016, collected from multiple sampling points, included parameters like pH, EC, TDS, TH, $Na^+$, $Ca^{2+}$, $Mg^{2+}$, $Cl^-$, $SO_4^2$, $NO_3^-$, and $PO_4^{3-}$. GWQI was calculated by weighting parameters against WHO standards, while GIS mapped seasonal and spatial quality variations. PCA identified key factors driving quality changes, with the first component (69.7–83.84% variance) linking salinity (EC, TDS, TH) and nutrient pollution ($NO_3^-$, $PO_4^{3-}$) to agricultural practices and evaporation, and the second (17.15–30.3% variance) reflecting $K^+$, $SO_4^{2-}$, $Na^+$, $Mg^{2+}$, and $Cl^-$, inversely related to TDS due to dilution. GWQI zonation showed good-to-excellent quality (0–50) in spring 2015, declining in autumn (50–75) due to evaporation and agricultural inputs, and improving in winter 2016 from rainfall infiltration. Eastern regions consistently exhibited poorer quality. The study highlights natural (evaporation, mineral dissolution) and anthropogenic (agriculture, contamination) influences on groundwater quality, with relative stability between 2015 and 2016 but notable seasonal variability. The integrated PCA, GWQI, and GIS approach, applied for the first time in this region, offers a robust framework for identifying critical zones and guiding localized management strategies. Biannual data and high-resolution mapping enhance methodological rigor, providing new insights into hydrogeochemical challenges and a dynamic tool for sustainable groundwater management.

## 1. Introduction

Groundwater provides approximately one-third of the world's freshwater supply and plays a pivotal role in sustaining domestic, industrial, and agricultural water demands, especially in arid and semi-arid regions where surface water resources are limited and unevenly distributed [1]. In countries such as Iran, which face both water scarcity and unequal spatial distribution of water resources, the management of groundwater quality is critically important. However, despite its strategic importance, rapid population growth, widespread industrialization, and intensive agricultural practices have led to the degradation and pollution of groundwater in many parts of the world. The consumption of contaminated groundwater poses serious threats to public health and can increase the prevalence of water-related diseases [2-4]. Accordingly, groundwater quality deterioration has become one of the principal global challenges to achieving sustainable development. In this context, multi-parameter evaluation and qualitative zoning through

* Corresponding author.
*E-mail addresses:* m.morsali@sci.ui.ac.ir (M. Morsali).

https://doi.org/10.22080/ceas.2025.29622.1026
**ISSN:** 3092-7749/© 2025 The Author(s). Published by University of Mazandaran.

How to cite this article: Ghaderi Khorasgani, M., Zarif Sanayei, H., Morsali, M., Toghyani, S. Multi-parameter assessment and qualitative zoning of groundwater resources to identify critical quality areas using a GIS approach. Civil Engineering and Applied Solutions. 2025;1(2): 74–87. doi:10.22080/ceas.2025.29622.1026.

Geographic Information Systems (GIS) have emerged as effective tools for identifying critical quality zones and supporting evidence-based water resource management. GIS facilitates spatial analysis and the visualization of complex hydrogeochemical datasets, enabling decision-makers to detect vulnerable areas with greater precision. The following section reviews relevant national and international studies related to this research focus.

## 2. Literature review

In Iran, due to the country's heavy reliance on groundwater resources, numerous studies have been conducted to assess groundwater quality and delineate spatial patterns using GIS. Li et al. [5], utilizing data from 27 wells in Abadeh County and applying the Schuler diagram alongside various interpolation techniques, demonstrated that kriging with exponential and circular variograms yielded the most accurate results for drinking water quality zoning. Similarly, Maghami et al. [6] evaluated groundwater quality in the Malayer Plain using the Water Quality Index (WQI) and GIS-based interpolation methods such as kriging and Inverse Distance Weighting (IDW). Their findings indicated that IDW was more suitable for interpolating parameters like electrical conductivity (EC) and total dissolved solids (TDS) in areas with uniformly distributed data, emphasizing the importance of selecting appropriate interpolation methods to enhance the accuracy of quality maps. Sadeghi et al. [7] analyzed groundwater chemistry data from the Amol–Babol Plain (1986–2009) using FAO standards and GIS-based zoning. Their results revealed that pollution was more critical near industrial zones and densely populated cities, with contamination levels increasing during low-discharge years. The use of sampled water quality data for delineating pollution zones has also been explored in several studies [8-16].

At the international level, recent advancements in remote sensing, machine learning, and GIS have significantly enhanced groundwater quality assessment and zoning. Tabrizi et al. [17], in a study conducted in southern India, employed WQI and GIS to evaluate groundwater quality in a semi-arid region. By analyzing physicochemical parameters such as TDS, nitrate, and heavy metals, they identified critical zones and demonstrated the effectiveness of GIS in visualizing and managing water quality data. In another study, Adimalla et al. [3] used GIS and geostatistical methods to map groundwater quality in Dhaka, Bangladesh. By analyzing 15 quality parameters and applying statistical techniques such as the Mann-Kendall trend test and Sen's Slope estimator, they assessed spatiotemporal variations and highlighted GIS as a powerful tool for detecting pollution trends. Karim et al. [18] investigated groundwater quality in the Achhnera region of Agra, India, by collecting and analyzing 50 samples. Their study employed WQI and Principal Component Analysis (PCA) to identify pollution sources. Results indicated that most samples were alkaline and unsuitable for drinking, underscoring the necessity of water treatment prior to consumption.

A comprehensive review of previous studies on groundwater quality degradation and pollutant sources reveals an escalating global challenge, particularly in arid and semi-arid regions such as Iran. While multiple factors contribute to this trend, anthropogenic activities, including overexploitation, agricultural runoff, urban wastewater discharge, and industrial effluents, play a central role in groundwater contamination. Given the rising demand for water across agricultural and industrial sectors, and in the absence of integrated quantitative and qualitative management strategies, the downward trend in groundwater quality is expected to accelerate. This issue is especially critical in Chaharmahal and Bakhtiari province, where declining precipitation, population growth, and the province's strategic role in supplying water to central and southwestern Iran amplify the urgency. Increased dependence on groundwater for agriculture, drinking, and industry, coupled with the widespread use of chemical fertilizers and rising volumes of municipal, industrial, and livestock wastewater, has intensified groundwater pollution in the region.

In summary, population growth, agricultural expansion, and increased wastewater generation are the primary drivers of groundwater contamination in Chaharmahal and Bakhtiari. Therefore, a precise and up-to-date assessment of groundwater quality in this province is essential. This study aims to identify critical and polluted zones by evaluating groundwater quality using a comprehensive set of physicochemical indicators. Its innovative approach integrates multiple indices with GIS-based zoning techniques to provide a holistic and accurate depiction of groundwater status. This integrated methodology enables the identification of spatial pollution patterns and prioritization of management actions, thereby contributing to the development of effective strategies for groundwater protection and restoration.

The following points highlight the innovative contributions of this study:

- Integrates multiple physicochemical indices with GIS-based zoning for a comprehensive groundwater quality assessment.
- Provides a novel spatial analysis of pollution patterns to identify critical and polluted zones accurately.
- Enhances groundwater management by prioritizing targeted protection and restoration strategies.

## 3. Methodology

### *3.1. Study area*

Chaharmahal and Bakhtiari Province, covering an area of 16,533 km² in western Iran (Fig. 1), is situated within the Zagros Mountain range. The province's highest elevation is Zardkuh Peak at 4,536 m above sea level, while its lowest point lies at the confluence of the Bazoft and Armand rivers in the Margak region, at 800 m. Geologically, most of the province belongs to the Zagros structural zone, with its northern part extending into the Sanandaj–Sirjan metamorphic belt. This mountainous region, located between the internal foothills of the Zagros and Isfahan Province, is part of Iran's central plateau. Due to the region's young orogenic activity and the presence of active fault systems, it is prone to natural hazards such as floods, earthquakes, and landslides. Fig. 1 also presents the province's digital elevation model (DEM) and land use classification.

Thanks to its high-altitude terrain and exposure to moisture-laden Mediterranean air masses, the province receives relatively high precipitation. Despite comprising only 1% of Iran's land area, it contributes approximately 10% of the country's total water resources. Snowfall and rainfall in the province's highlands feed two of Iran's most significant perennial rivers: the Karun and the Zayandeh-Rud, with respective catchment areas of 13,800 km² and 2,720 km². The Zayandeh-Rud is the only permanent river in Iran's central plateau, while the Karun is the country's largest river. However, both rivers face serious threats due to extensive dam construction and unsustainable inter-basin water transfers to provinces such as Yazd, Isfahan, and Kerman. With an average elevation of 2,153 m, the province features a rugged topography of hills and intermontane plains separated by mountain ridges. It includes 16 peaks exceeding 3,500 m in elevation (Fig. 1). These mountains extend from the northwest to the southeast of the province, gradually decreasing in height toward the east and into Isfahan Province. This transition leads to the formation of relatively broad plains such as Shahrekord, Farsan, Sefiddasht, Borujen–Faradonbeh, Kiar, Shalamzar, Gandoman–Boldaji, and Lordegan. Collectively, these plains account for approximately 24% of the province's area and are composed of alluvial deposits that provide favorable conditions for agriculture. However, the aquifers beneath these plains are limited in capacity and have been severely overexploited. As a result, all plains in the province are currently classified as either critical, restricted, or restricted zones for groundwater extraction. Of the ten major plains, four-Borujen-Faradonbeh, Javanmardi, Sefiddasht, and Shahr-e Kord are in a critical restricted state, while the remaining four Kiar, Lordegan, Gandoman–Boldaji, and Falard are designated as restricted.

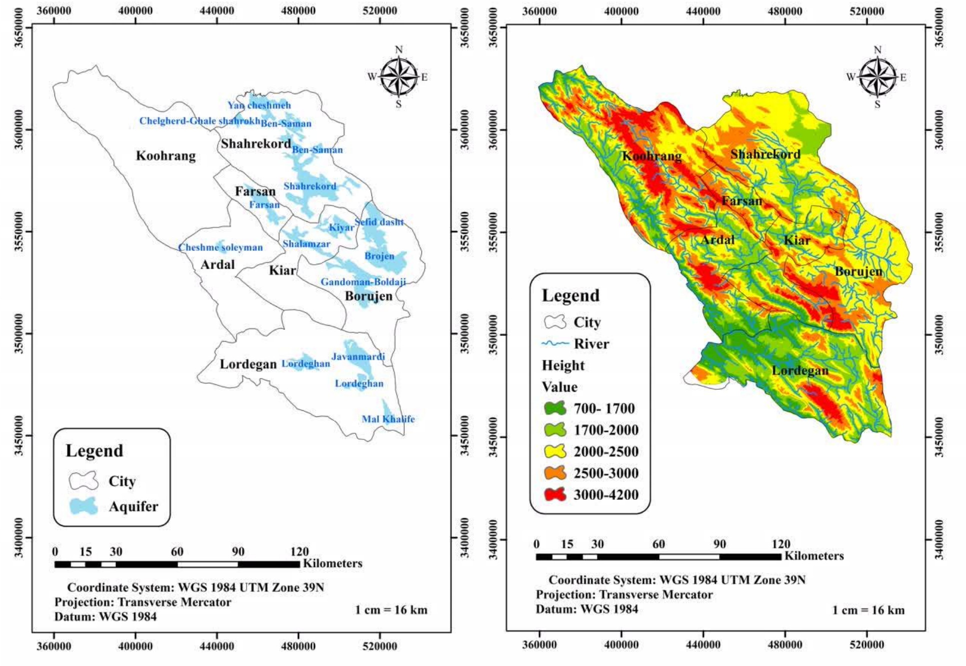


**Fig. 1. Location of the study area with topographic variation.**

### *3.2. Data collection and compilation*

The sustainable development of water resources in any country is highly dependent on the availability of comprehensive databases encompassing both baseline data and accurate quantitative and qualitative analyses. These databases play a pivotal role in infrastructure planning, water use optimization, and the effective management of this vital resource. Only through rigorous analysis of the multiple components of the hydrological cycle, including hydrological, climatic, and environmental characteristics, can the actual capacity of water resources be assessed to meet the demands of sustainable economic and social development, thereby enabling the successful implementation of national infrastructure projects. Chaharmahal and Bakhtiari Province, owing to its unique hydroclimatological features, hosts a network of high-discharge rivers and valuable watershed systems. However, existing investigations reveal that the available data on the quantity and quality of water resources in this region suffer from significant limitations and deficiencies. A large portion of the data has been recorded over short time intervals, and the lack of continuous monitoring at measurement stations has compromised the accuracy and reliability of the information. To evaluate groundwater quality in the study area, the measurement and analysis of key water quality parameters were deemed essential. In this study, data about the physical and chemical characteristics of groundwater including EC, pH, total hardness (TH), TDS, sodium adsorption ratio (SAR), sulfate ($SO_4^{2-}$), chloride ($Cl^-$), sodium percentage (Na%), potassium ($K^+$), magnesium ($Mg^{2+}$), and calcium ($Ca^{2+}$) were examined for the years 2015 and 2016 (Table 1). These data were obtained in coordination with the Chaharmahal and Bakhtiari Regional Water Authority and collected using standard laboratory instruments such as portable EC and pH meters, as well as titration methods for hardness and ionic concentrations. Sampling and analytical protocols were conducted per the standards of the World Health Organization (WHO) and the Food and Agriculture Organization (FAO) to ensure data accuracy. Although the data used in this study were sourced from reputable institutions, limitations such as the absence of continuous monitoring at certain stations and the potential inclusion of reconstructed datasets may have affected the precision of the results. To mitigate these limitations, incomplete records were excluded, and only validated data were used in the analyses. Nevertheless, it should be noted that reconstructed datasets, even when developed using rigorous scientific methodologies, cannot fully match the quality of real-time measurements, and thus, their reliability remains inherently constrained.

**Table 1. Number of sampling points in the study area.**

| Year | Spring | Summer | Autumn | Winter | Total |
|---|---|---|---|---|---|
| 1394 | 110 | 22 | 64 | 0 | 196 |
| 1395 | | 37 | 77 | 62 | 180 |

*3.3. Study approach*

To assess the groundwater quality across the plains of Chaharmahal and Bakhtiari Province, a total of 196 samples in 2015 and 180 samples in 2016 were collected from various water sources, including operational wells, springs, and qanats. Sampling locations were purposefully selected to ensure adequate spatial coverage across the province's diverse plains. The geographic coordinates of each sampling point were recorded using a GPS device and mapped in ArcGIS 10.8 (Fig. 2). Sampling was conducted during both wet and dry seasons of the study years to capture potential seasonal variations in water quality. The collected data were statistically analyzed using SPSS version 24. Initially, the Kolmogorov–Smirnov test was applied to assess the normality of data distribution. Descriptive statistics, including mean, median, standard deviation, minimum, and maximum, were calculated for each parameter. To evaluate interannual differences between 2015 and 2016, a paired t-test was employed.

Additionally, Pearson correlation analysis was conducted to identify relationships between key water quality parameters, such as the correlation between EC and TDS. For spatial distribution mapping of groundwater quality parameters, ArcGIS 10.8 was used. The Kriging interpolation method was selected due to its high accuracy in modeling spatially heterogeneous data. This method was applied to generate zoning maps for key parameters such as EC, TDS, SAR, and pH, delineating areas with suitable and unsuitable water quality for drinking and agricultural purposes. To evaluate groundwater suitability for drinking, the results were compared with WHO standards, and for agricultural use, with FAO guidelines. The key water quality indicators assessed in this study include:

- EC: Indicates water salinity and its impact on agricultural use.
- SAR: Assesses irrigation suitability based on sodium's effect on soil permeability.
- TH: Reflects concentrations of calcium and magnesium, relevant to drinking and industrial use.
- TDS: A general indicator of water quality for both drinking and irrigation consumption.
- pH and Major Ions ($SO_4^{2-}$, $Cl^-$, $Na^+$, $K^+$, $Mg^{2+}$, $Ca^{2+}$): Used to evaluate chemical equilibrium and environmental implications.

These indicators were assessed per international standards and local hydrogeological conditions to support informed decision-making for optimal groundwater resource management.

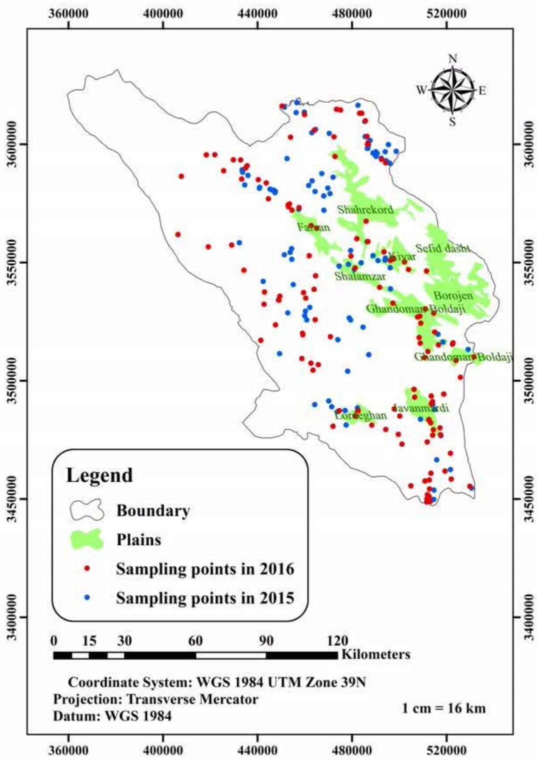


**Fig. 2. Spatial distribution of sampling points in the study area during 2015 and 2016.**

### *3.4. Groundwater quality index (GWQI)*

The Groundwater Quality Index (GWQI) is one of the most widely used indices for qualitative zoning of water resources. Compared to other existing models, it presents fewer limitations and is frequently adopted by researchers due to its simplicity and the accessibility of required quality parameters. This index is calculated based on values of key indicators such as pH, TDS, $Cl^-$, $Ca^{2+}$, $Mg^{2+}$, $SO_4^{2-}$, $HCO_3^-$, and $Na^+$. GWQI is a reverse-scale index, meaning that as the level of contamination increases, the index value decreases. The method integrates the cumulative effect of multiple water quality parameters into a single numerical value that reflects the overall groundwater quality. The number and type of parameters used in the calculation are flexible and adaptable depending on the study objectives and data availability. Typically, WHO drinking water standards are employed as reference thresholds in GWQI computation, making the index a reliable indicator of potability. A critical aspect of GWQI calculation is the identification of parameters with the highest and lowest sensitivity to the index outcome. To address this, a sensitivity analysis is applied to determine the influence of each parameter on the final GWQI score [19].

$$GWQI = \sum SI_i = \sum (W_i \times q_i) = \sum ((\frac{w_i}{\sum_{i=1}^{n} w_i}) \times (\frac{C_i}{S_i} \times 100)) \quad (1)$$

where the variables are defined as follows:

- $W_i$: Weight of parameter $i$
- $q_i$: Quality rating of parameter $i$, calculated by normalizing the measured concentration
- $C_i$: Measured concentration of parameter $i$
- $S_i$: Standard or guideline value for parameter $i$, based on international benchmarks such as the WHO for drinking water or the FAO for agricultural use

Two main approaches are employed for the evaluation of the GWQI:

**a) GIS-based method**

In this approach, groundwater quality data such as EC, pH, TDS, TH, SAR, and concentrations of major ions are collected from sampling points. These data are processed using ArcGIS 10.8, and spatial distribution maps for each parameter are generated through geostatistical interpolation techniques, such as Kriging. The individual parameter maps are then integrated using assigned relative weights, reflecting the significance of each parameter for the intended use (drinking or irrigation). The final GWQI map is created based on this weighted overlay. GWQI values are normalized within a 0–100 range, where values near 0 indicate excellent water quality and those near 100 represent poor quality. In addition, sensitivity analysis is conducted to evaluate the impact of excluding individual parameter maps on the accuracy of the GWQI. This method enables the spatial identification of groundwater quality patterns and critical zones, making it highly effective for regional-scale water resource management.

**b) Data-driven method**

The data-driven approach relies on the analysis of point-based field data for assessing groundwater quality. It computes the GWQI as a unitless score ranging from 1 to 100 based on observed concentrations. Due to its relative simplicity and minimal dependency on advanced geospatial tools, this method is suitable for studies with limited computational resources or a focus on non-spatial analysis. In this approach, lower GWQI values correspond to better groundwater quality, while higher values indicate deterioration. The classification of groundwater based on GWQI is presented in Table 2.

**Table 2. Classification of groundwater quality based on GWQI.**

| Water Quality Classification | Index Value |
|---|---|
| Excellent (Suitable for all uses) | 0-25 |
| Good (Suitable for drinking and irrigation with minor limitations) | 25-50 |
| Moderate (Use with caution for specific purposes) | 50-75 |
| Poor (Requires treatment for drinking or has agricultural limitations) | 75-100 |
| Very Poor | 100-125 |
| Unsuitable (Unusable without extensive treatment) | More than 125 |

### *3.5. Graphical methods for groundwater quality assessment*

Most approaches employed in groundwater quality studies are graphical, where the results of water sample analyses are presented using diagrams such as Piper, Chadha, Stiff, Wilcox, and Schoeller plots. One limitation of graphical methods lies in the number of samples and variables they can effectively handle. Moreover, graphical techniques cannot distinguish between sample groups or test for similarity among them. In contrast, statistical methods do not suffer from these constraints and are increasingly applied in groundwater quality investigations. However, a drawback of statistical methods is that they do not directly convey the chemical composition of the samples, and their results are not as readily interpretable in the context of hydrochemical processes and trends. Therefore, combining graphical and statistical approaches can retain the strengths of each while minimizing their limitations. In this study, the Piper trilinear diagram was utilized to classify groundwater types and hydrochemical facies. The use of triangular diagrams for hydrochemical data representation was first introduced by Hill and later developed by Piper, whose diagram became widely adopted globally. In Piper diagrams, ions are plotted as percentages of milliequivalents per liter in two separate triangles representing cations and anions. These values are then projected into a central diamond field for comparative analysis. The Piper diagram enables the simultaneous comparison of a large number of analyzed samples. The size of plotted circles on the diagram may also represent TDS content. Overall, the Piper diagram presents the chemical characteristics of water based on the relative concentrations of its constituents [20].

Following the collection and preprocessing of statistical data, groundwater quality zoning maps were developed using ArcGIS 10.8. The GIS is an advanced computational platform for acquiring, storing, analyzing, and visualizing spatial data. It offers a unique capability to integrate, organize, and interpret spatial relationships among various parameters. In GIS, all data possess geographic attributes and can be effectively visualized. One of its numerous applications lies in the field of public health [21], where the spatial linkage of environmental and health data facilitates informed decision-making [22]. Identifying geographic areas at risk is considered a fundamental step in implementing preventive and therapeutic measures to mitigate risk factors and their societal consequences. Based on previous research and the outcomes of related studies, the strengths and limitations of each method can be assessed to provide actionable insights for future investigations. Owing to the versatility and effectiveness of GIS in various domains, it is also employed in the qualitative zoning of groundwater resources.

### *3.6. Determination of spatial distribution patterns of indicators*

Understanding and comparing environmental phenomena inherently require their quantification or measurement. In principle, point-based data derived from sampling sites are insufficient on their own, and it is essential to spatially extend and generalize such information. To spatially interpolate point data considering both the spatial and temporal variability of each parameter, models are needed that can simulate the behavior of the studied variable at unsampled locations. Among these, geostatistical methods, such as Kriging, Co-Kriging, Thin Plate Spline Smoothing (TPSS), and Weighted Moving Average (WMA), are of considerable importance due to their incorporation of spatial correlation and the underlying spatial structure of the data. In geostatistics, not only the value of a measured variable but also the spatial coordinates of the sampling point are taken into account. Thus, it becomes possible to jointly analyze the spatial location and the corresponding quantitative attribute of each observation.

Spatial visualization of raw environmental data using maps within a GIS facilitates more efficient and comprehensive communication of information compared to numerical indices alone. Moreover, due to the irregular nature of spatial variation, describing all changes solely through numerical indices is often unfeasible. Therefore, to describe and represent the spatial variability of a given parameter, it is necessary to estimate its values at unsampled points using the known data from sampled locations [23]. In this study, spatial autocorrelation analysis, interpolation of unsampled locations, and the generation of prediction maps and zoning layers were conducted using ArcGIS 10.8. The process of estimating the values of a continuous variable in areas where direct measurements are unavailable is referred to as interpolation. In essence, interpolation visualizes continuous spatial variation as a well-defined surface. It plays a fundamental role in the mapping, analysis, and interpretation of two-dimensional environmental data. Various interpolation techniques exist for estimating spatially and temporally variable parameters. These methods differ primarily in how they assign weights to known surrounding observations to estimate values at unknown locations. Based on prior studies and to extend point-based data into spatially continuous representations while ensuring computational efficiency and avoiding unnecessary complexity, the Kriging geostatistical method was selected for use in this study.

### *3.7. Factor analysis*

One of the statistical methods used for analyzing data sets is Factor Analysis (FA). This method is similar to regression analysis; however, in FA, the observed variables are regressed on latent (unobservable) factors. The primary objective of factor analysis is to explain the covariance structure among variables through a limited number of random, unobserved quantities known as factors. In this approach, variables grouped within the same factor exhibit high intercorrelation, while those in separate groups show relatively low correlation. Several techniques exist for extracting factors within the framework of factor analysis, which are discussed further below. Among multivariate statistical techniques, Principal Component Analysis (PCA) is commonly used to identify the key parameters influencing groundwater quality, and in this study, it was applied to determine the most influential parameters in assessing groundwater quality in the plains of Chaharmahal and Bakhtiari Province.

Among the spatial analysis methods, PCA is frequently employed for dimensionality reduction of input datasets. PCA aims to extract a smaller number of components that can capture the majority of the variance present in a large dataset, a process known as data reduction. This approach is particularly useful when the researcher does not wish to involve all original variables in the analysis but still requires the information they contain. PCA is a general technique for factor extraction that seeks to identify linear combinations of the variables that explain the maximum possible variance. Once the first principal component is extracted, its associated variance is removed, and the next principal component that explains the largest remaining variance is identified. This iterative process continues until the optimal number of components is determined. This method is also known as the principal axes method, which results in the creation of orthogonal (uncorrelated) axes [24].

PCA is considered one of the most powerful multivariate statistical tools and is particularly effective when dealing with large volumes of data, as it reduces the number of input variables without significant information loss. Initially, the input data were standardized using the appropriate formula in SPSS software. In the next step, the suitability of the dataset for PCA was assessed using the Kaiser-Meyer-Olkin (KMO) measure and Bartlett's test of sphericity. To enhance the interpretability of the relationships between input variables and extracted components and to better distinguish their groupings, Varimax rotation was applied.

## 4. Results and discussions

### *4.1. Comparative analysis of groundwater quality parameters*

To evaluate the groundwater quality status over a two-year period based on measured quality parameters, the statistical characteristics of the data were first presented for the summer season of 2015 and 2016 in Tables 3 and 4. The analysis of groundwater quality data during the summer of 2015 and 2016 across the Chaharmahal and Bakhtiari plains revealed that the average pH declined from 7.65 in 2015 to 7.22 in 2016, approaching a more neutral condition. This reduction in average pH in 2016 may be associated with increased inputs of organic or inorganic pollutants, such as wastewater infiltration or agricultural fertilizers. However, the pH levels in both years remained within the WHO recommended range for drinking water (6.5–8.5), indicating suitability for this purpose.

EC and TDS increased from 448.64 µS/cm and 299.05 mg/L in 2015 to 466.46 µS/cm and 310.35 mg/L in 2016, respectively, indicating rising salinity levels in some areas. The increase in EC in 2016 suggests a higher concentration of dissolved ions or possible intrusion of saline water (e.g., from agricultural runoff or industrial wastewater). The broader EC range observed in 2016 reflects localized zones with elevated salinity, which may impose constraints on agricultural use (FAO standard: EC < 700 µS/cm for salt-sensitive crops). The rise in TDS aligns with the EC trend, indicating an increase in overall dissolved solids. Despite this, TDS concentrations in both years remained below the WHO threshold for drinking water (< 1000 mg/L), though values nearing 663 mg/L in some areas could pose limitations for sensitive crops.

TH exhibited a significant increase from 176.98 to 274.97 mg/L, mainly due to a marked rise in magnesium concentration (from 4.43 to 19.59 mg/L), while calcium and sodium levels decreased. The substantial rise in hardness in 2016 is likely related to increased concentrations of calcium and magnesium ions. In some locations, TH values approached the upper limit of the “hard” classification range (200–500 mg/L), which may affect drinking water palatability and lead to sedimentation issues in industrial applications.

The decrease in mean sodium concentration in 2016 may indicate reduced saline water intrusion or changes in agricultural practices. However, the wider concentration range suggests the presence of localized high-sodium zones, which should be evaluated for their potential to cause soil sodicity in agricultural lands.

A decline in potassium levels and reduced variability in 2016 (standard deviation of 0.015) could imply lower agricultural fertilizer inputs. The sharp rise in magnesium alongside a reduction in calcium may reflect underlying geological variations or differences in the sampled water sources, which could affect total hardness and warrant further hydrochemical investigation. The increase in sulfate concentration in 2016 may stem from agricultural activities (e.g., use of sulfate-based fertilizers) or wastewater infiltration, though values remained within the WHO guideline for drinking water (< 250 mg/L). The observed decrease in chloride concentration in 2016 may be indicative of reduced salinity or diminished saline water intrusion, with values in both years remaining acceptable for potable use.

$NO_3^-$ concentration showed a significant increase from an average of 1.61 to 15.16 mg/L, emerging as a potential concern for drinking water in some areas. The marked rise in nitrate levels in 2016 suggests possible contamination from nitrogenous fertilizers or sewage. Concentrations exceeding 39.1 mg/L in certain locations approach the WHO limit (50 mg/L), highlighting the need for stricter monitoring and management.

**Table 3. Descriptive statistics of groundwater quality parameters in the summer season of 2015.**

| Parameters | Minimum | Maximum | Mean | SD | Variance |
|---|---|---|---|---|---|
| PH | 7.51 | 7.88 | 7.66 | 0.1 | 0.01 |
| EC(µs/cm) | 228 | 556 | 448.64 | 120.3 | 14475.19 |
| TDS(mg/l) | 153 | 369 | 299.04 | 79.01 | 6242.9 |
| TH | 160.2 | 280.8 | 176.98 | 34 | 1158.1 |
| K | 0.1 | 1.3 | 0.51 | 0.292 | 0.086 |
| Na | 1 | 26 | 18.77 | 7.98 | 63.71 |
| Mg | 1 | 10.5 | 4.43 | 3.57 | 12.7 |
| Ca | 47.4 | 97.4 | 63.57 | 12.6 | 159.13 |
| $Sio_3$ | 0.23 | 0.93 | 0.46 | 0.23 | 0.054 |
| Br | 0.2 | 0.4 | 0.33 | 0.055 | 0.003 |
| $PO_4$ | 0.1 | 0.7 | 0.32 | 0.28 | 0.076 |
| $NO_2$ | 1 | 8.2 | 6.21 | 0.24 | 5.03 |
| $NO_3$ | 1.2 | 4.5 | 1.61 | 0.66 | 0.44 |
| $SO_4$ | 1 | 50 | 14.23 | 14.11 | 199.32 |
| Cl | 21.8 | 49.7 | 34.67 | 6.78 | 46 |
| F | 0.03 | 0.1 | 0.059 | 0.016 | 0 |

**Table 4. Statistical characteristics of groundwater quality parameters in summer 2016.**

| Parameters | Minimum | Maximum | Mean | SD | Variance |
|---|---|---|---|---|---|
| PH | 6.5 | 7.5 | 7.22 | 0.62 | 0.069 |
| EC(µs/cm) | 193 | 1004 | 466.46 | 190.28 | 36208.42 |
| TDS(mg/l) | 128 | 663 | 310.35 | 126.42 | 15982.4 |
| TH | 180 | 524.8 | 274.96 | 83.2 | 6923 |
| K | 0.38 | 0.41 | 0.387 | 0.015 | 0 |
| Na | 1.69 | 41.39 | 12.3 | 8.53 | 72.75 |
| Mg | 12.6 | 27.56 | 19.59 | 7.53 | 56.67 |
| Ca | 6.73 | 38 | 21.87 | 12.88 | 165.9 |
| $NO_2$ | 0 | 0.14 | 0.051 | 0.033 | 0.001 |
| $NO_3$ | 0 | 39.1 | 15.16 | 10.81 | 116.84 |
| $SO_4$ | 5.6 | 30 | 17.8 | 17.25 | 297.68 |
| Cl | 10 | 43 | 31 | 18.25 | 333 |

### *4.2. Hydrochemical analysis of groundwater using the Piper diagram*

Based on the chemical composition of groundwater samples collected during autumn and winter of 2016, the hydrogeochemical facies and groundwater types were interpreted using the Piper diagram (Figs. 3 and 4). In autumn 2016, the dominant hydrochemical facies was Ca–$HCO_3$ (calcium–bicarbonate), indicating fresh groundwater typically associated with karstic origins or interaction with carbonate formations. The prevailing water type was calcium–bicarbonate, although some samples exhibited a tendency toward mixed facies such as Ca–Na–$HCO_3$–Cl, likely due to elevated sodium and chloride concentrations. The formation of this facies during autumn can be attributed to the following factors:

- The presence of carbonate formations (e.g., limestone and dolomite) in the region enhances calcium and bicarbonate concentrations through mineral dissolution.
- Relatively high concentrations of chloride and sodium in certain locations, potentially linked to agricultural return flows (e.g., chloride- or sodium-based fertilizers) or wastewater infiltration.
- Carbonate mineral dissolution and ion exchange processes within the aquifer system, contributing to the development of the Ca–$HCO_3$ facies.

In winter 2016, the dominant hydrochemical facies shifted to Mg–$HCO_3$ or Ca–Mg–$HCO_3$, reflecting increased magnesium concentrations alongside bicarbonate. In some areas with elevated nitrate and sodium, mixed facies such as Mg–Na–$HCO_3$–Cl were also observed. The prevailing water types were magnesium–bicarbonate or calcium–magnesium–bicarbonate, with certain samples trending toward Mg–$HCO_3$–$SO_4$ facies due to increased nitrate and sulfate levels. The formation of these facies in winter can be explained by:

- Elevated magnesium concentrations, likely resulting from the dissolution of dolomitic minerals ($CaMg(CO_3)_2$) within the aquifer.
- Increased nitrate levels, probably due to the infiltration of nitrogen-based fertilizers or agricultural/urban wastewater. Elevated sulfate may also be linked to the use of sulfate-containing fertilizers.
- Changes in groundwater flow patterns or reduced aquifer recharge, potentially leading to higher ion concentrations during the winter season.

### *4.3. Factors influencing groundwater quality variation based on PCA*

To identify and interpret the key factors controlling groundwater quality variation, PCA was performed on the dataset of water quality parameters. This multivariate statistical method reduces the dimensionality of the dataset by extracting a set of uncorrelated components (principal components), each representing a group of interrelated parameters that together explain a significant portion of the total variance. The factor loadings for each parameter on each component indicate the strength and direction of its contribution to the formation of that component. Based on the average water quality data collected over the two-year study period, the factor loadings and the percentage of variance explained by each principal component were extracted for the years 2015 and 2016, as shown in Tables 5 and 6. The PCA results for the year 2015 are interpreted as follows:

**Principal Component 1 (PC1)** in Table 5 accounts for the largest share of variance (84.83%) and is dominated by strong negative loadings for pH, $PO_4$, $NO_3$, Cl, and F, and strong positive loadings for EC, TDS, TH, Na, Ca, $SiO_3$, Br, and Mg. Based on this component, the hydrogeochemical variations observed in the aquifer can be attributed to the following:

- **Salinity and Hardness Effects**: The strong positive loadings for EC, TDS, TH, Na, Ca, and Mg indicate the critical role of evaporative concentration, mineral dissolution (e.g., carbonates and sulfates), and the intrusion of saline water or mineralized surface water in governing groundwater hydrogeochemistry. These may be linked to agricultural activities, irrigation, or seawater intrusion in coastal areas.

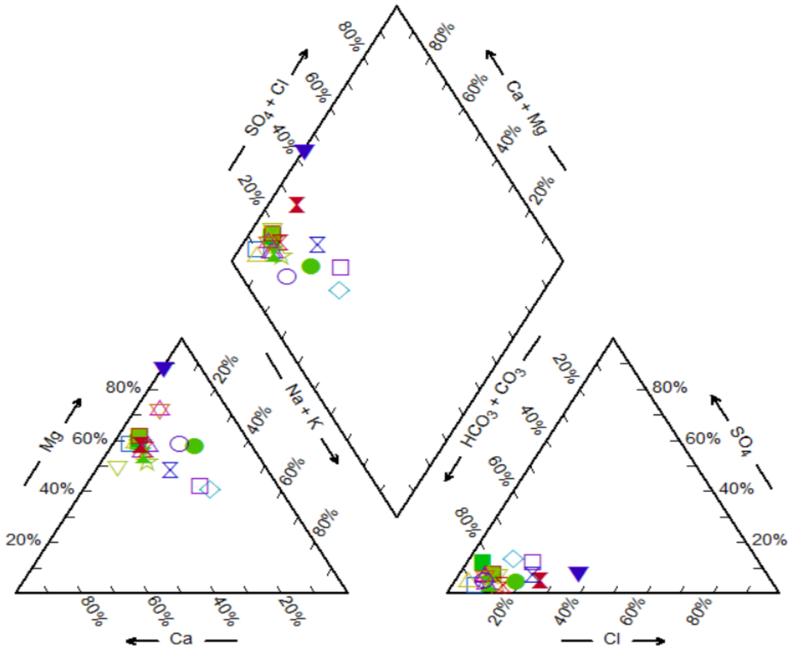


**Fig. 3. Piper diagram of water samples in autumn 2016.**

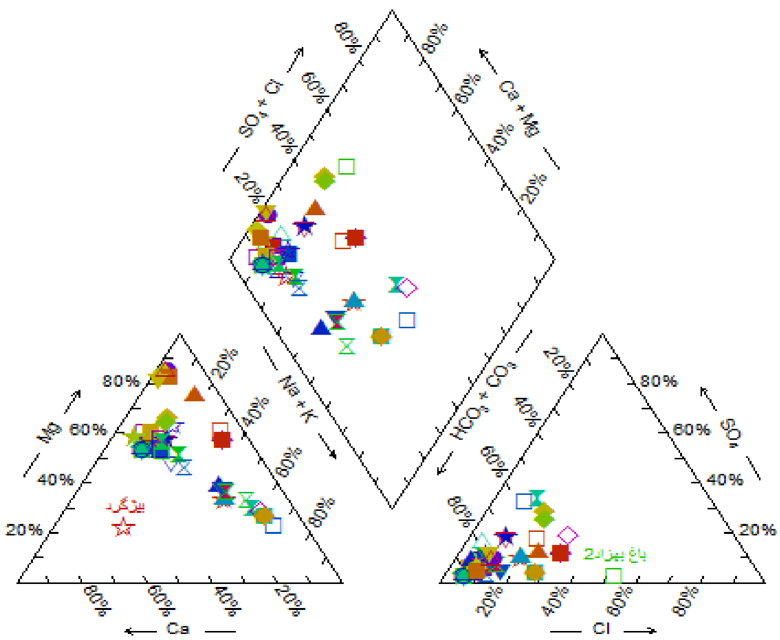


**Fig. 4. Piper diagram of water samples in winter 2016.**

- **Influence of Specific Ions and Pollution Sources**: The positive loadings for $SiO_3$ and Br may reflect natural geogenic sources such as silicate minerals or deeper groundwater inputs, while the strong negative loadings for Cl and F suggest potential anthropogenic contamination (e.g., wastewater discharge or agricultural fertilizers) or localized geochemical conditions.
- **pH and Nutrient Interactions**: The strong negative loading for pH suggests an inverse relationship between acidity and salinity/hardness parameters, which could be attributed to buffering effects from dissolved minerals or biological activities such as organic matter degradation.
- The negative loadings for $PO_4$ and $NO_3$ may indicate agricultural contamination sources (e.g., nitrogen and phosphorus-based fertilizers) that inversely correlate with salinity, possibly due to dilution effects or adsorption in soil matrices.

Overall, PC1 represents a dominant hydrogeochemical gradient characterized by increased salinity/hardness (positive loadings) versus reduced pH and nutrient levels (negative loadings). This pattern likely results from the interaction between mineral dissolution, evaporation, saline water intrusion, and anthropogenic pollution. For example, elevated EC and TDS may result from surface water infiltration or evaporation in arid zones, whereas reduced pH and elevated nutrient indicators may reflect domestic wastewater or agricultural runoff. In essence, PC1 illustrates a prevailing hydrogeochemical process involving increased groundwater salinity and hardness due to mineral dissolution and saline intrusion, counteracted by nutrient pollution (phosphate and nitrate) and associated pH variations. To interpret this component more precisely, local variables such as soil type, climate, and land use must also be considered.

**Principal Component 2 (PC2)** explains a smaller share of the variance (15.17%) and is primarily characterized by high positive loadings for potassium (K: 0.960) and sulfate ($SO_4$: 0.976). The origin of groundwater quality variations represented by this component can be explained as follows:

- The strong loading for potassium indicates its significant influence within PC2, which could be linked to the weathering of potassium-bearing minerals (e.g., K-feldspar, mica) in the aquifer matrix or the leaching of potassium-rich water (e.g., from agricultural fertilizers). Elevated potassium levels may thus be associated with agricultural practices or selective weathering processes.
- The very high loading for sulfate highlights its importance in this component, which may originate from the dissolution of sulfate minerals (e.g., gypsum or anhydrite) or the oxidation of sulfide minerals (e.g., pyrite) in the subsurface. Elevated $SO_4$ concentrations may also reflect anthropogenic inputs such as industrial or agricultural runoff containing sulfate compounds.

Generally, this component appears to represent a secondary hydrogeochemical gradient governed by potassium and sulfate concentrations, in contrast to the dominant salinity and hardness parameters in PC1. PC2 may reflect localized processes such as selective mineral weathering, infiltration of sulfate-rich water, or point-source pollution. Moreover, the strong correlation between K and $SO_4$ may indicate a common source (e.g., potassium-sulfate fertilizers) or specific geochemical interactions within the groundwater system. Thus, PC2 represents a secondary hydrogeochemical process influenced by potassium and sulfate sources either geogenic (e.g., mineral weathering) or anthropogenic (e.g., fertilizer use or industrial discharge).

**Table 5. Varimax-rotated principal component matrix of groundwater physicochemical parameters for the year 2015.**

| Component | PH | EC | TDS | TH | K | Na | Mg | Ca |
|---|---|---|---|---|---|---|---|---|
| 1 | -0.997 | 0.998 | 0.994 | 0.984 | -0.28 | 0.918 | 0.989 | 0.997 |
| 2 | 0.08 | 0.06 | -0.107 | 0.176 | 0.96 | -0.396 | 0.15 | 0.079 |
| **Component** | **Sio3** | **Br** | **PO4** | **NO2** | **NO3** | **SO4** | **Cl** | **F** |
| 1 | 0.965 | 0.961 | -0.96 | -0.995 | 0.999 | 0.218 | -0.951 | 0.958 |
| 2 | -0.263 | -0.277 | -0.276 | 0.102 | 0.036 | 0.976 | 0.309 | -0.285 |

In 2016, the status of the dominant components is as follows:

As shown in Table 6, PC1 accounts for 69.7% of the total variance. This component is characterized by strong negative loadings for EC, TDS, TH, Ca, and Cl, and strong positive loadings for pH, K, Na, $PO_4$, $HCO_3$, $SO_4$, Cl, and $NO_3$. The strong negative loadings suggest that carbonate and sulfate mineral dissolution (e.g., calcite) and saline water intrusion play a significant role in degrading groundwater quality. These processes may be associated with evaporation, surface water infiltration, or irrigation practices. Meanwhile, the strong positive loadings for pH, $PO_4$, and $NO_3$ indicate the influence of acid–base buffering conditions and nutrient-related pollution. The rise in pH may result from natural buffering mechanisms or biological activity, such as the decomposition of organic matter. The presence of $PO_4$ and $NO_3$ may reflect contamination from agricultural fertilizers or domestic wastewater. Positive loadings for Na, K, $HCO_3$, and $SO_4$ highlight diverse geochemical sources, including mineral dissolution (e.g., sodium carbonate or sulfate minerals) and the infiltration of bicarbonate-enriched water. The appearance of Cl with both negative and positive loadings in this component may suggest multiple pollution sources.

The similarity of the PC1 loading pattern to that of 2015 with comparable contributing parameters suggests relative consistency in the dominant hydrogeochemical processes. However, the change in loading direction for parameters such as Cl (from negative to positive) may indicate shifts in water sources, intensified anthropogenic activities (e.g., agriculture or industry), or climatic variations (e.g., rainfall or drought) during 2016.

In summary, PC1 in 2016 reflects the combined influence of salinity, hardness, and mineral dissolution, along with nutrient pollution (phosphate and nitrate) and pH fluctuations. This pattern likely stems from agricultural practices, saline water intrusion, and environmental interactions. A comparison with 2015 indicates the persistence of these processes, with minor changes in the source and dominance of specific ions.

PC2 explains 30.3% of the total variance in 2016 and shows strong positive loadings for Na, Mg, $SO_4$, and Cl, along with a strong negative loading for TDS. The high positive loadings for Na and Mg point to the influence of mineral dissolution processes, such as the weathering of halite, dolomite, or chlorite, or the infiltration of ion-rich waters. This may be related to the weathering of evaporite rocks or the percolation of surface water.

The strong positive loadings for $SO_4$ and Cl suggest dissolution of sulfate-bearing minerals (e.g., gypsum) or chloride-rich sources (e.g., halite), as well as possible contamination from saline water intrusion or anthropogenic sources, such as wastewater discharge or agricultural runoff. This pattern may reflect the influence of evaporation or human activity on groundwater chemistry. The strong negative loading for TDS suggests an inverse relationship between TDS and the positively loaded ions, possibly indicating selective enrichment of Na, Mg, $SO_4$, and Cl under conditions of localized dilution (e.g., rainfall events or infiltration of lower-TDS water). Thus, PC2 appears to represent a secondary geochemical gradient, primarily associated with the selective dissolution of Na, Mg, $SO_4$, and Cl-bearing minerals and an opposing trend in total salinity. This may result from the interplay of weathering, localized evaporation, and the mixing of groundwater with chemically distinct waters. The negative loading of TDS could reflect dilution events during the 2016 period.

**Table 6. Rotated component matrix for physicochemical parameters in 2016.**

| Component | PH | EC | TDS | TH | K | Na | Mg |
|---|---|---|---|---|---|---|---|
| 1 | 0.999 | -0.976 | -0.975 | -0.983 | 0.9 | 0.419 | -0.352 |
| 2 | -0.053 | 0.217 | 0.224 | -0.184 | 0.436 | 0.908 | 0.936 |
| **Component** | **Ca** | **PO4** | **NO2** | **NO3** | **HCO3** | **SO4** | **Cl** |
| 1 | -0.973 | 0.984 | 0.34 | 0.959 | 0.971 | 0.694 | -0.47 |
| 2 | 0.233 | -0.175 | -0.941 | -0.285 | -0.239 | 0.72 | 0.883 |

### *4.4. Aquifer quality assessment based on GWQI*

By applying weighted values to the collected groundwater quality variables, GWQI was calculated and seasonally zoned across Chaharmahal and Bakhtiari Province, enabling both spatial and temporal evaluation of groundwater quality. As outlined in Section 3.4, Part a, this study utilized point data collected from water resources within the aquifer to calculate the Groundwater Quality Index (GWQI) and map its distribution across the aquifer. The GWQI was computed using the parameters pH, EC, TDS, $Cl^-$, $Ca^{2+}$, $Mg^{2+}$, $SO_4^{2-}$, TH, $NO_3$, K, and $Na^+$, each assigned different weights based on their respective impacts and sensitivity to aquifer quality degradation. The weights assigned to the parameters, along with their respective standard values, have been incorporated into the manuscript as Table 7. The arrangement of weights and their relative importance were determined based on recommendations from previous studies, and no sensitivity analysis was conducted for individual parameters.

**Table 7. Standard values (WHO (2017)) of quality parameters used in GWQI calculation and their assigned weights.**

| Parameter* | pH | EC | TDS | TH | K | Na | Mg | Ca | SO4 | Cl | NO3 |
|---|---|---|---|---|---|---|---|---|---|---|---|
| **Standard Value** | 8.5 | 750 | 500 | 200 | 12 | 0.419 | 50 | 75 | 250 | 250 | 50 |
| **Assigned Weight** | 4 | 4 | 4 | 2 | 2 | 4 | 2 | 2 | 4 | 3 | 5 |

* The units of all parameters, except for pH (dimensionless) and EC (μs/cm), are in mg/L.

The analysis of GWQI variations in spring 2015 indicates that large portions of the study area, particularly in the central and eastern regions, fall within the "good to excellent" quality range. This favorable condition is likely attributed to spring rainfall infiltration. As illustrated in Fig. 5, groundwater quality during this season predominantly lies within the 0–50 range, reflecting a relatively favorable aquifer status. In contrast, the GWQI map for autumn 2015 reveals a relative decline in groundwater quality compared to spring, especially in areas where GWQI values range between 50 and 75. This seasonal degradation may be linked to increased evaporation, reduced precipitation, and intensified agricultural activities. The latter, particularly the use of fertilizers, could have contributed to elevated concentrations of nitrate ($NO_3^-$) and phosphate ($PO_4^{3-}$), a trend consistent with the positive loadings for these parameters observed in the earlier PCA results.

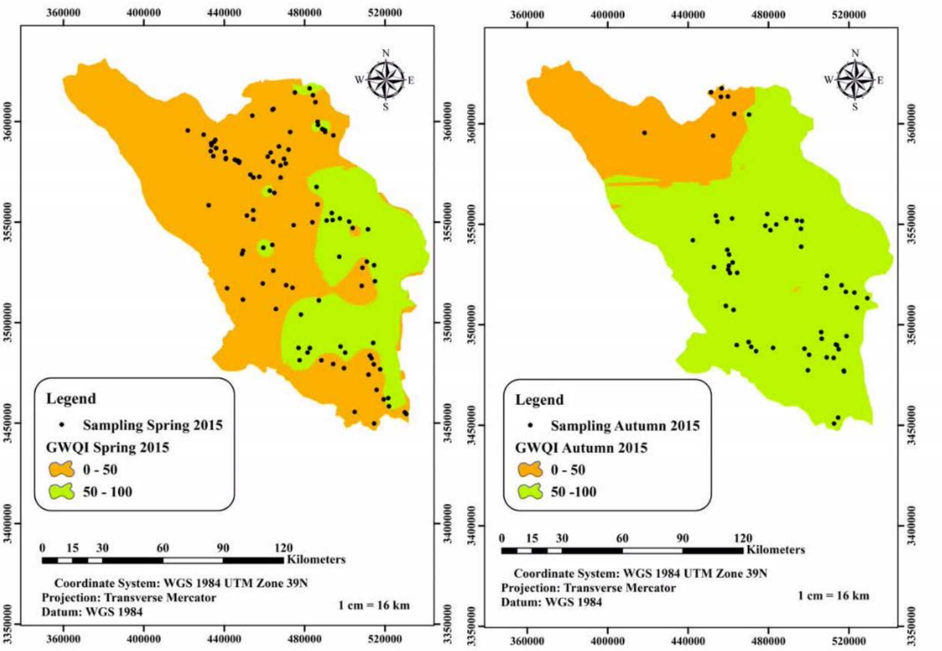


**Fig. 5. Seasonal zoning map of GWQI in spring and autumn 2015.**

The analysis of groundwater quality variations in 2016 reveals that during the winter season, due to limited rainfall infiltration and the presence of anthropogenic pollution in urban areas, low-quality patches emerged in the eastern parts of the aquifer (Fig. 6). Overall, however, a relative stabilization and improvement in groundwater quality compared to the previous year was observed, based on the GWQI.

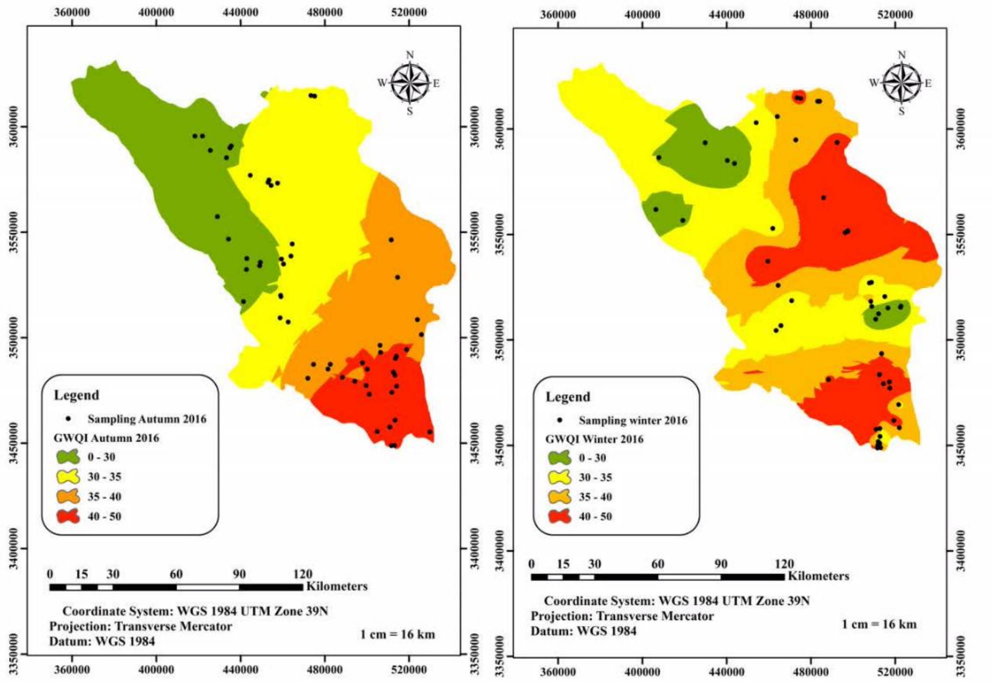


**Fig. 6. Seasonal zoning map of GWQI in autumn and winter 2016.**

## 5. Conclusions

Based on qualitative data collected over two years (2015–2016), the groundwater quality status across the aquifers of Chaharmahal and Bakhtiari Province was assessed, and the potential sources of quality variation were identified. The key findings are summarized as follows:

- The increase in TDS in 2016 correlates with elevated EC levels, indicating a rise in dissolved salts. Although the values remain within acceptable limits for drinking, they may pose challenges for salt-sensitive agricultural activities.
- A notable increase in water hardness, primarily attributed to elevated magnesium concentrations, may adversely affect domestic usage (taste) and industrial applications (scaling issues).
- The decline in mean sodium concentration suggests a potential reduction in saline water intrusion or changes in agricultural irrigation practices. However, the wider range of sodium values in 2016 highlights localized hotspots of high sodium concentration, raising concerns over sodicity hazards in agricultural soils.
- The observed reduction and homogenization of potassium levels in 2016 may indicate a decrease in agricultural fertilizer input.
- The increase in magnesium and concurrent decrease in calcium concentrations could be attributed to geological variations or differences in water source lithology at the sampling locations.
- The elevated sulfate levels may stem from agricultural activities, such as the application of sulfate-based fertilizers or wastewater infiltration. Nevertheless, the concentrations remain within safe limits for drinking water.
- The decline in chloride concentrations may reflect a reduction in salinity levels or a diminished influx of saline water, with values deemed suitable for drinking in both years.
- A significant increase in nitrate was identified in some locations, representing a potential health risk for drinking water and indicating the necessity for enhanced nitrate monitoring.
- Hydrogeochemical analysis of groundwater during the autumn and winter seasons of 2016 revealed seasonal variability in dominant hydrochemical facies: Ca-$HCO_3$ type in autumn and Mg-$HCO_3$ or Ca-Mg-$HCO_3$ types in winter. This shift may result from interactions between groundwater and carbonate/dolomitic formations, surface pollutant infiltration (especially in winter), and changes in groundwater flow dynamics, contributing to facies heterogeneity in the aquifer.
- PCA of groundwater quality data indicated that the first principal component (explaining up to 83.84% of variance in 2015 and 69.7% in 2016) is associated with salinity, hardness, and nutrient-related contamination (nitrate and phosphate), inversely influenced by pH and mineral dissolution, and predominantly linked to agricultural activities and evaporation.

The second component (17.15% in 2015 and 30.3% in 2016) reflects the presence of specific ions (K, $SO_4$, Na, Mg, Cl) and TDS dilution effects, pointing to mineral weathering and saline water intrusion. The persistence of these patterns across both years, despite minor shifts in ion sources, emphasizes the need for local-scale groundwater management and monitoring.

## 6. Recommendations for future research

- Enhanced nitrate monitoring: Given the significant increase in nitrate concentrations, reaching values near the WHO permissible limit, it is essential to conduct frequent and seasonally distributed monitoring across all sampling sites.
- Detailed hydrogeochemical analysis: To better understand the drivers of ion concentration changes, particularly for Mg, Ca, and Na, more comprehensive hydrogeochemical evaluations are required. These should include ion ratio analysis, saturation index calculations, and hydrochemical modeling.
- Pollution source identification: To determine the origins of nitrate and sulfate, detailed investigations into agricultural practices (types and application rates of fertilizers) and the presence of wastewater sources are crucial. This includes assessment of sewage systems, septic tanks, and agricultural drainage systems.
- Agricultural impact assessment: Given the increased TDS and localized high sodium levels, it is necessary to assess the implications for regional crop production. This could involve soil testing, monitoring of plant toxicity or deficiency symptoms, and consultation with agronomic experts.
- Soil sodicity risk evaluation: Due to the wide range of sodium values, it is recommended to compute the SAR in different areas and assess the sodicity hazard. If risk is confirmed, mitigation strategies such as soil amendments and improved drainage systems should be implemented.
- Human health risk assessment: Considering the increase in hardness and nitrate, evaluating the potential public health impacts is imperative. This could involve reviewing health records for waterborne diseases, conducting epidemiological studies, and issuing health advisories for the local population.
- Comparison with historical datasets: To gain a more comprehensive understanding of groundwater quality trends, it is essential to compare the two-year dataset with long-term historical records. This comparison can reveal temporal patterns and assist in identifying underlying causes of quality changes.

## Statements & Declarations

*Author contributions*

**Milad Ghaderi Khorasgani:** Conceptualization, Methodology, Formal analysis, Resources, Writing - Original Draft.

**Hamed Reza Zarif Sanayei:** Resources, Writing - Original Draft.

**Masoud Morsali:** Conceptualization, Formal analysis, Resources, Writing - Original Draft.

**Saeed Toghyani:** Conceptualization, Writing - Original Draft.

*Funding*

The authors received no financial support for the research, authorship, and/or publication of this article.

*Data availability*

The data presented in this study will be available on interested request from the corresponding author.

*Declarations*

The authors declare no conflict of interes.

# References

[1] Shaikh, H., Gaikwad, H., Kadam, A., Umrikar, B. Hydrogeochemical characterization of groundwater from semiarid region of western India for drinking and agricultural purposes with special reference to water quality index and potential health risks assessment. Applied Water Science, 2020; 10: 204. doi:10.1007/s13201-020-01287-z.

[2] Zhang, Y., Wu, J., Xu, B. Human health risk assessment of groundwater nitrogen pollution in Jinghui canal irrigation area of the loess region, northwest China. Environmental Earth Sciences, 2018; 77: 1-12. doi:10.1007/s12665-018-7456-9.

[3] Adimalla, N., Dhakate, R., Kasarla, A., Taloor, A. K. Appraisal of groundwater quality for drinking and irrigation purposes in Central Telangana, India. Groundwater for Sustainable Development, 2020; 10: 100334. doi:10.1016/j.gsd.2020.100334.

[4] Diédhiou, M., Ndoye, S., Celle, H., Faye, S., Wohnlich, S., Le Coustumer, P. Hydrogeochemical appraisal of groundwater quality and its suitability for drinking and irrigation purposes in the west central Senegal. Water, 2023; 15: 1772. doi:10.3390/w15091772.

[5] Li, P., He, X., Guo, W. Spatial groundwater quality and potential health risks due to nitrate ingestion through drinking water: a case study in Yan'an City on the Loess Plateau of northwest China. Human and ecological risk assessment: an international journal, 2019; 25: 11-31. doi:10.1080/10807039.2018.1553612.

[6] Maghami, Y., Ghazavi, R., Vali, A. A., Sharafi, S. Evaluation of spatial interpolation methods for water quality zoning using GIS Case study, Abadeh Township. Geography and Environmental Planning, 2011; 22: 171-182. doi:20.1001.1.20085362.1390.22.2.10.3.

[7] Sadeghi, S. H., Ghasemieh, H., Moemeni Damaneh, Javad, Mosavi, S. H. Irrigation and municipal water quality zoning by GIS. Irrigation and Water Engineering, 2016; 6: 128-137.

[8] Heidarzadeh, N., Moezzi, M. Groundwater quality analysis in Amol-Babol plain and zoning of sodium using GIS. Journal of Environmental Science and Technology, 2018; 4: 81-93. doi:10.22034/jest.2019.13703.

[9] Alimoradi, H., Rouhimoghaddam, E., Khaleghi, M., Bameri, A. Predicting and zoning of groundwater quality using geographical information system (GIS) models and machine learning methods (case study: Zahedan plain). Hydrogeology, 2023; 7: 43-60. doi:10.22034/hydro.2022.48571.1250.

[10] Jaafarzadeh, M. S., Moghaddamnia, A., Joodavi, A., Ahmadi, A. Assessment of the quality of Salmas aquifer and mapping of areas with pollution potential. Journal Of Iranian Water Engineering Research, 2023; 2: 35-56. doi:10.22034/ijwer.2024.482845.1056.

[11] Chitsazan, M., Tabari, M. M. R., Eilbeigi, M. Analysis of temporal and spatial variations in groundwater nitrate and development of its pollution plume: a case study in Karaj aquifer. Environmental Earth Sciences, 2017; 76: doi:10.1007/s12665-017-6677-7.

[12] Nemati, M., Tabari, M., Hosseini, S. A., Javadi, s. Identification of Factors Affecting Nitrate Contamination in Ardabil Plain Aquifer Using Statistical Methods. Water and Irrigation Management, 2023; 13: 527-550. doi:10.22059/jwim.2022.343545.995.

[13] Nemati, M., Tabari, M. M. R., Hosseini, S. A., Javadi, S. A Novel Approach Using Hybrid Fuzzy Vertex Method-MATLAB Framework Based on GMS Model for Quantifying Predictive Uncertainty Associated with Groundwater Flow and Transport Models. Water Resources Management, 2021; 35: 4189-4215. doi:10.1007/s11269-021-02940-1.

[14] Chitsazan, M., Eilbeigy, M., Mohammad Rezapour Tabari, M. Evaluation of Groundwater Nitrate Pollution Based on Main Components and Factor Analysis (Case Study: Karaj Plain Aquifer). Journal of Ecohydrology, 2018; 5: 1119-1133. doi:10.22059/ije.2018.256758.870.

[15] Tabari, M. M. R., Kabiri, S. M. Groundwater quality assessment using entropy weighted osculating value and set pair analysis methods (case study, SARAYAN plain). 2019; 21: 99-112.

[16] Tabari, M. M. R., Salehi, D. P. Groundwater Contaminantion Analysis Using Fuzzy-Topsis, Case Study: ZANJAN Plain. Journal of Environmental Science and Technology, 2020; 22: 101-116.

[17] Tabrizi, F., Movahed, E., Ojaqlou, H. Quality zonation of nitrate concentration for underground sources of drinking water in Lavasan City using Geographic Information System (GIS). Environmental Studies, Natural Resources and Sustainable Development Journal, 2020; 14: 45-52.

[18] Karim, M. R., Arham, M. A., Shorif, M. J. U., Ahsan, A., Al-Ansari, N. GIS based geostatistical modelling and trends analysis of groundwater quality for suitable uses in Dhaka division. Scientific Reports, 2024; 14: 17449. doi:10.1038/s41598-024-66567-z.

[19] Ali, S., Verma, S., Agarwal, M. B., Islam, R., Mehrotra, M., Deolia, R. K., Kumar, J., Singh, S., Mohammadi, A. A., Raj, D. Groundwater quality assessment using water quality index and principal component analysis in the Achnera block, Agra district, Uttar Pradesh, Northern India. Scientific Reports, 2024; 14: 5381. doi:10.1038/s41598-024-56056-8.

[20] Eftekhari, M., Eslaminezhad, S. A., Haji Elyasi, A., Akbari, M. Geostatistical Evaluation with Drinking Groundwater Quality Index (DGWQI) in Birjand Plain Aquifer. Environment and Water Engineering, 2021; 7: 267-278. doi:10.22034/jewe.2021.256731.1464.

[21] Azari, T., Tabari, M. M. R. An integrated approach based on HFE-D, GIS techniques, GQI SWI, and statistical analysis for the assessment of potential seawater intrusion: coastal multilayered aquifer of Ghaemshahr-Juybar (Mazandaran, Iran). Environmental Science and Pollution Research, 2024; 31: 13335-13371. doi:10.1007/s11356-024-31967-1.

[22] Stewart, O. T., Carlos, H. A., Lee, C., Berke, E. M., Hurvitz, P. M., Li, L., Moudon, A. V., Doescher, M. P. Secondary GIS built environment data for health research: Guidance for data development. Journal of transport & health, 2016; 3: 529-539. doi:10.1016/j.jth.2015.12.003.

[23] James, P., Jankowska, M., Marx, C., Hart, J. E., Berrigan, D., Kerr, J., Hurvitz, P. M., Hipp, J. A., Laden, F. "Spatial energetics": integrating data from GPS, accelerometry, and GIS to address obesity and inactivity. American journal of preventive medicine, 2016; 51: 792-800. doi:10.1016/j.amepre.2016.06.006.

[24] Mohammadyari, F., Aghdar, H., Basiri, R. Zoning groundwater quality for drinking using geo-statistical methods Case Study: Arid Regions in Mehran and Dehloran. "Sepehr" Quarterly Scientific-Research Journal of Geographic Information, 2017; 26: 199-208. doi:10.22131/sepehr.2017.25737.